Article

Discovery Medicine 2024; 36(180): 82–90
https://doi.org/10.24976/Discov.Med.202436180.7

XRCC1 rs1799782 Promotes DNA Damage Repair in Lung Cancer Cells by Enhancing Its Binding to *FOXA1* to Facilitate *FOXA1*-Mediated Transcription of *XRCC1*

Cunlai Xu[1,†], Yuling Li[1,†], Jiongwei Pan[1], Shuanghu Wang[2], Zaiting Ye[3], Xiaoping Cai[1], Hao Zheng[1], Zhangyong Yin[1], Zhuo Cao[1,*]

[1]Respiratory Department, The Sixth Affiliated Hospital of Wenzhou Medical University, 323000 Lishui, Zhejiang, China
[2]Department of Medicine, Lishui People's Hospital, 323050 Lishui, Zhejiang, China
[3]Radiology Department, The Sixth Affiliated Hospital of Wenzhou Medical University, 323000 Lishui, Zhejiang, China
*Correspondence: caozhuo_cz@163.com (Zhuo Cao)
[†]These authors contributed equally.
Published: 20 January 2024

Background: *X-ray repair cross complementing 1* (*XRCC1*) rs1799782 polymorphism is associated with an increased risk of lung cancer (LC). The aim of this study is to analyze the underlying biological mechanisms.
Methods: Dual luciferase reporter assay was utilized to verify the impact of *XRCC1* polymorphism upon promoter activity of *XRCC1*. Cell counting kit-8 (CCK-8) assay, colony formation assay, senescence-associated beta-galactosidase (SA-β-gal) staining, and immunofluorescent staining were used to assess the viability, proliferation, senescence, and DNA damage of LC cells. Senescence-related proteins (cyclin dependent kinase inhibitor 1A (P21) and eukaryotic translation elongation factor 1-alpha (EF1A)) were quantified by Western blot. Chromatin immunoprecipitation was applied to validate the binding affinity of *forkhead box A1* (*FOXA1*) and *XRCC1*. *FOXA1*-specific short hairpin RNA (sh*FOXA1*) was used to perform the rescue assay.
Results: In LC cells, *XRCC1* rs1799782 promoted viability and proliferation, inhibited senescence, and resulted in upregulation of EF1A as well as downregulation of P21 and *phosphorylated H2A.X variant histone* (γ*H2AX*). *XRCC1* rs1799782 promoted *FOXA1*-mediated transcription of *XRCC1* through enhancing its binding to *FOXA1*. sh*FOXA1* counteracted the effects of *XRCC1* rs1799782 upon the viability, proliferation, and senescence of LC cells.
Conclusions: *XRCC1* rs1799782 promotes DNA damage repair in LC cells through enhancing its binding to *FOXA1*, which facilitates *FOXA1*-mediated transcription of *XRCC1*.

Keywords: *forkhead box A1*; lung cancer; rs1799782; senescence; *X-ray repair cross complementing 1*

Introduction

Lung cancer (LC) has been one of the most prevalent cancer types in most countries, whose risk factors include genetic susceptibility, smoking, environment, occupational exposure, and pulmonary infection [1]. Previous studies have shown that LC has unlimited proliferation and immune escape abilities, largely due to changes in tumor-related genes [2]. These changes include somatic mutation, gene amplification, gene deletion, and single nucleotide polymorphism (SNP). At present, the genetic variation in *epidermal growth factor receptor* (*EGFR*), *KRAS proto-oncogene, GTPase* (*KRAS*), and other genes has been considered a biomarker of LC, and corresponding targeted drugs are rapidly being developed [3]. Therefore, it is of great value to explore the genetic variation in LC cells for the diagnosis and treatment of LC.

Notably, *X-ray repair cross complementing 1* (*XRCC1*) polymorphism is related to LC risk [4]. *XRCC1*, as an important component in the base excision repair (BER) system, is localized on human chromosome 19q13.2, and its main function is to participate in BER and DNA single-strand break repair after DNA damage caused by ion radiation and chemical mutagenesis [5]. At present, *XRCC1* has a total of eight SNP sites, of which three are the most common, namely codons 194 (Arg194Trp, rs1799782), 280 (Arg280His, rs25489) and 399 (Arg399Gln, rs25487) [6]. For LC patients, the *XRCC1* gene polymorphism can change protein activity and affect DNA repair ability, thus regulating the development of cancer.

It is worth noting that the SNP of the *XRCC1* gene can also regulate transcription activity by binding to transcription factors [7]. In a study by Qingtao Meng *et al.* [8], *XRCC1* rs3213245 can enhance the binding of *Sp1 transcription factor* (*SP1*) to the *XRCC1* promoter, thereby promoting the development of cervical cancer. However, it is unclear whether the SNP of *XRCC1* plays a carcino-

genic role in the development of LC through similar effects. Using Haplorg Version 4.2 (https://pubs.broadinstitute.org/mammals/haploreg/haploreg.php) (Cambridge, MA, USA) analysis, we found that *XRCC1* rs1799782 may bind to *forkhead box A1* (*FOXA1*). In many different types of cancers, including prostate, breast, and bladder cancers, *FOXA1* is overexpressed and has carcinogenic properties [9]. Of note, *FOXA1* has been shown to be upregulated in LC and could promote the tumorigenicity of LC cells [10]. Other potential biomarkers of LC risk include *phosphorylated H2A.X variant histone* (*γH2AX*), which marks sites of DNA damage [11], *eukaryotic translation elongation factor 1-alpha* (*EF1A*), which is involved in apoptosis and tumor progression [12], and *cyclin dependent kinase inhibitor 1A* (*P21*), a marker of cellular senescence [13]. Therefore, we postulated that *XRCC1* rs1799782 promotes DNA damage repair and the development of LC by enhancing its binding to transcription factor *FOXA1*.

Materials and Methods

Cell Culture

LC cell line A549 (IM-H113) (Immocell, Xiamen, China) was cultured in A549 cell specific medium (IM-H113-1, Immocell, Xiamen, China) at 37 ℃ with 5% CO_2. The cells were authenticated by short tandem repeat (STR) analysis and exhibited a negative result for mycoplasma contamination.

Cell Transfection

XRCC1 wild-type (XRCC1-Wild-G) and mutant (XRCC1-Mutant-A) plasmids were constructed by Genepharma (Shanghai, China). The +/-100 bp base before and after the mutation site was inserted into the PGL3-basic plasmid (E1751, Promega, Madison, WI, USA). *FOXA1*-specific short hairpin RNA (sh*FOXA1*-1, target sequence: 5′-CAAACCGTCAACAGCATAATA-3′; sh*FOXA1*-2, target sequence: 5′-ATGATCCACAAGTGTATATAT-3′; sh*FOXA1*-3, target sequence: 5′-TAGTTTGTGGAGGGTTATTTA-3′) and its negative control (shNC) were purchased from Genepharma (Shanghai, China). LC cells were shifted into 6-well plates (5×10^5 cells/well) for culture. When cells grew to about 70% confluence, Lipo8000 Transfer Reagent (C0533, Beyotime, Shanghai, China) mixed with plasmids was added into each well and incubated for an additional 24 hours.

Dual Luciferase Reporter Assay (DLRA)

After LC cells were put into 24-well plates and cultivated for 24 hours, the XRCC1-Wild-G, XRCC1-Mutant-A, PGL3-basic plasmid or PRL plasmid (E2231, Promega, Madison, WI, USA) was transfected into LC cells using Lipo8000 Transfer Reagent. 24 hours later, the relative luciferase activity was tested using the Dual Luciferase Reporter Assay (DLRA) System (E1910, Promega, Madison, WI, USA).

Cell Counting Kit-8 (CCK-8) Assay

The evaluation of cell viability was accomplished by cell counting kit-8 (CCK-8) kit (B34302, Bimake, Shanghai, China). LC cells plated onto 96-well plates (3×10^3 cells per well) were cultivated for 24 hours. Next, CCK-8 reagent was added and cells were incubated for 2 hours. Finally, the absorbance (450 nm) was gauged by a microplate reader (HBS-ScanX, DeTiebio, Nanjing, China).

Colony Formation Assay

Cells (100 per well) in 6-well plates were grown in complete medium for 14 days. After fixation using 4% paraformaldehyde (MM1504, Maokangbio, Shanghai, China) and staining by crystal violet (BB44577, Beibokit, Hangzhou, China), the number of cell colonies was counted under an optical microscope (N300M, Yongxin, Henan, China).

Senescence-Associated Beta-Galactosidase (SA-β-gal) Staining

The senescence-associated beta-galactosidase (SA-β-gal) staining kit (BB4151, Beibokit, Shanghai, China) was used to assess the senescence of LC cells. Specifically, cells were transferred to a 12-well plate for 24 hours of cultivation, and then rinsed by phosphate buffered saline (PBS, BB43074, Beibokit, Shanghai, China). Thereafter, cells were soaked in 4% paraformaldehyde and blended with SA-β-gal staining solution. 24 hours later, cells expressing SA β-gal were blue-green, and the images were captured by camera.

Western Blot

LC cells were immersed in radioimmunoprecipitation (RIPA) lysis buffer (BB3201, Beibokit, Shanghai, China) to obtain total protein, and then protein quantification was accomplished using a bicinchoninic acid (BCA) Assay Kit (BB3401, Beibokit, Hangzhou, China). Next, the protein samples were electrophoresed using sodium dodecyl-sulfate polyacrylamide gel electrophoresis (SDS-PAGE), and electrophoretically moved onto a Polyvinylidene fluoride (PVDF) membrane (1620177, Bio-Rad, Hercules, CA, USA). Subsequently, the membrane was mixed with 5% skimmed milk for blocking and then reacted with primary antibodies (Table 1) at 4 ℃ overnight. Afterwards, further reaction with secondary antibodies (Table 1) was implemented at room temperature for 1 hour. Glyceraldehyde-3-phosphate dehydrogenase (GAPDH) was used as an endogenous reference. The intensity of band signals was detected by enhanced chemiluminescence (ECL) reagent (BB3501, Beibokit, Hangzhou, China) and imaging Sys-

Table 1. Antibodies adopted in this study.

Name	Catalog	Molecular weight	Dilution	Manufacturer
P21	ab109520	21 kDa	1/2000	abcam, Cambridge, UK
EF1A	ab227824	50 kDa	1/1000	abcam, Cambridge, UK
GAPDH	ab8245	36 kDa	1/10000	abcam, Cambridge, UK
goat anti-rabbit	ab205718	—	1/2000	abcam, Cambridge, UK
goat anti-mouse	ab205719	—	1/2000	abcam, Cambridge, UK

P21, cyclin dependent kinase inhibitor 1A; EF1A, eukaryotic translation elongation factor 1-alpha; GAPDH, glyceraldehyde-3-phosphate dehydrogenase.

tem (SynGene, Frederick, MD, USA). The gray value of the bands was detected by Image J software (version 1.51w, NIH free software, Bethesda, MD, USA).

Immunofluorescent Staining

LC cells were plated in a 4-well plate and cultured for 24 hours. Prior to staining, cells were subjected to fixation using 4% paraformaldehyde for 10 minutes. After PBS washing, cells were immersed in 0.2% Triton X-100 (MS4311, Maokangbio, Shanghai, China) for 10 minutes of permeabilization, blended with 5% normal goat serum (MM0203, Maokangbio, Shanghai, China) for blocking, and probed with anti-phospho H2AX (S139) antibody (1:200, sc-517348, Santa Cruz Biotechnology, Santa Cruz, CA, USA) overnight at 4 ℃. Later, cells were reacted with a Fluor594-conjugated secondary antibody (red) (1:400, S0005, Affinity, Cincinnati, OH, USA), and counterstained with 4,6-diamidino-2-phenylindole (DAPI, blue, D1306, Thermo Fisher, Waltham, MA, USA). fluorescence microscope (Zeiss Axio Observer Z1, Zeiss, Jena, Germany) was employed to view the $\gamma H2AX$ foci. AxioVison 6.4 software (Carl Zeiss, Oberkochen, Germany) was used to capture the images. The speckle counting pipeline in CellProfiler (2.2.0, Broad Institute, Cambridge, MA, USA) was used to quantify $\gamma H2AX$ foci [14]. The foci count in the nucleus, multiplied by the mean integrated intensity of the foci within that nucleus, was defined as the $\gamma H2AX$ signal.

Quantitative Reverse Transcription Polymerase Chain Reaction (qRT-PCR)

Total RNA was isolated from LC cells by Trizol Reagent (MF0403, Maokangbio, Shanghai, China), 1 μg of which was used to synthesize cDNA with cDNA Synthesis Kit (1708891, Maokangbio, Shanghai, China). The expressions of target genes were assessed using qPCR Mix (B21202, Bimake, Shanghai, China) with specific primers (Table 2). The qPCR was completed in a Real-Time PCR System (7500, ThermoFisher, Waltham, MA, USA). The changes in mRNA expression were calculated by $2^{-\Delta\Delta CT}$ approach [15] and the data were normalized to GAPDH.

Chromatin Immunoprecipitation (ChIP)

Chromatin Immunoprecipitation (ChIP) assay was implemented under the help of ABclonal's ChIP Kit (RK20258, Abclonal, Beijing, China). Concretely, cells (2×10^7) were rinsed with ice-cold PBS, reacted with cell fixative for 10 minutes, and then centrifuged in Glycine solution for 5 minutes at 4 ℃. After the supernatant was discharged, cells were soaked in the cell lysate for resuspension, centrifuged at 5000 ×g for 5 minutes at 4 ℃, and then sonicated. Later, further centrifugation was carried out at 12,000 ×g for 10 minutes to remove nuclear debris. Thereafter, cells were reacted with anti-*FOXA1* antibody (1:1000, ab170933, abcam, Cambridge, UK) and anti-IgG antibody (1:1000, ab97051, abcam, Cambridge, UK). Then, the reaction solution was added into a tube containing Protein A/G magnetic beads, and the incubation was continued for 2 hours. After that, chromatin samples were obtained by elution and purified using a DNA purification kit (RK30100, ABclonal, Beijing, China). Finally, the experimental results were analyzed by qPCR.

Table 2. Primers utilized in this study.

Genes	Sequence (5′ –> 3′)
FOXA1 (human) Forward	GAAGACCGGCCAGCTAGAG
FOXA1 (human) Reverse	TTTGCACTGGGGGAAAGGTT
XRCC1 (human) Forward	ACCAAAACCAAGCCCACTCA
XRCC1 (human) Reverse	TATCGGATGAGTTTCCGCCG
GAPDH (human) Forward	CGACAGCAGCCGCATCTT
GAPDH (human) Reverse	CCAATACGACCAAATCCGTTG

FOXA1, *forkhead box A1*; *XRCC1*, *X-ray repair cross complementing 1*.

Statistical Analysis

The measurement data were displayed in the form of mean ± standard deviation. One-way analysis of variance was used to test differences among multiple groups, and the Tukey test was applied for post hoc analysis. Comparisons between two groups were analyzed by independent samples *t* test. In terms of statistical analyses, GraphPad 8.0 software (GraphPad Software, San Diego, CA, USA) was introduced. p values < 0.05 were considered statistically significant.

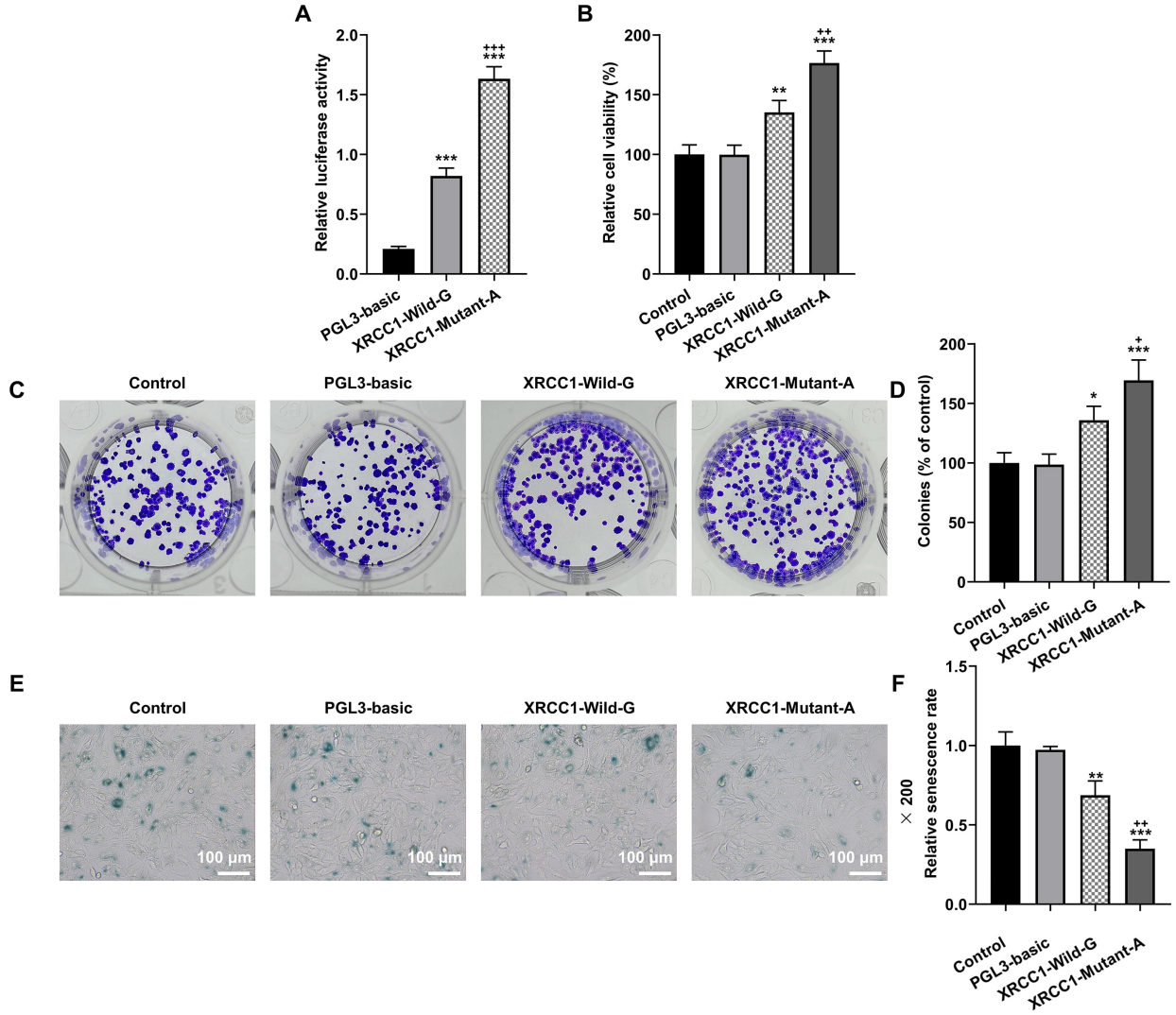

Fig. 1. Impacts of rs1799782 mutation of *XRCC1* upon the viability, proliferation and senescence of LC cells. XRCC1-Mutant-A refers to the mutant type, XRCC1-Wild-G indicates the wild type, and PGL3-basic plasmid is the control. (A) The impact of mutation on the activity of *XRCC1* promoter (dual luciferase reporter assay). (B) The viability of LC cells (CCK-8 assay). (C,D) The colony formation ability of LC cells (colony formation assay). (E,F) Cellular senescence (SA-β-gal staining assay; magnification: $\times$200, and scale bar = 100 μm). $^{*}p < 0.05$, $^{**}p < 0.01$, $^{***}p < 0.001$ vs. PGL3-basic. $^{+}p < 0.05$, $^{++}p < 0.01$, $^{+++}p < 0.001$ vs. XRCC1-Wild-G. Quantified values from at least three independent repeated experiments (n = 3) were depicted as mean $\pm$ standard deviation. LC, lung cancer; CCK-8, cell counting kit-8; SA-β-gal, senescence-associated beta-galactosidase.

Results

rs1799782 Promoted the Viability and Proliferation of LC Cells

Firstly, we investigated the effect of the rs1799782 mutation on the promoter activity of *XRCC1*, and the results indicated that the luciferase activity in the XRCC1-Mutant-A group was conspicuously stronger than that in the XRCC1-Wild-G group (Fig. 1A, $p < 0.001$). In addition, a series of cell function experiments were conducted in LC cells transfected with XRCC1-Mutant-A or XRCC1-Wild-G. XRCC1-Mutant-A or XRCC1-Wild-G was found to boost the viability and colony formation of LC cells, relative to PGL3-basic plasmid (Fig. 1B–D, $p < 0.05$). Moreover, increased cell viability and colonies were observed in the XRCC1-Mutant-A group, as compared with the XRCC1-Wild-G group (Fig. 1B–D, $p < 0.05$).

rs1799782 Inhibited Senescence and DNA Damage of LC Cells

Increased SA-β-gal activity is recognized as a biomarker of senescence. In XRCC1-Mutant-A or XRCC1-Wild-G group, the number of SA-β-gal^{+} cells was markedly lower than that in the PGL3-basic group (Fig. 1E,F, $p < 0.01$). Moreover, the XRCC1-Mutant-A group displayed fewer SA-β-gal^{+} cells than XRCC1-

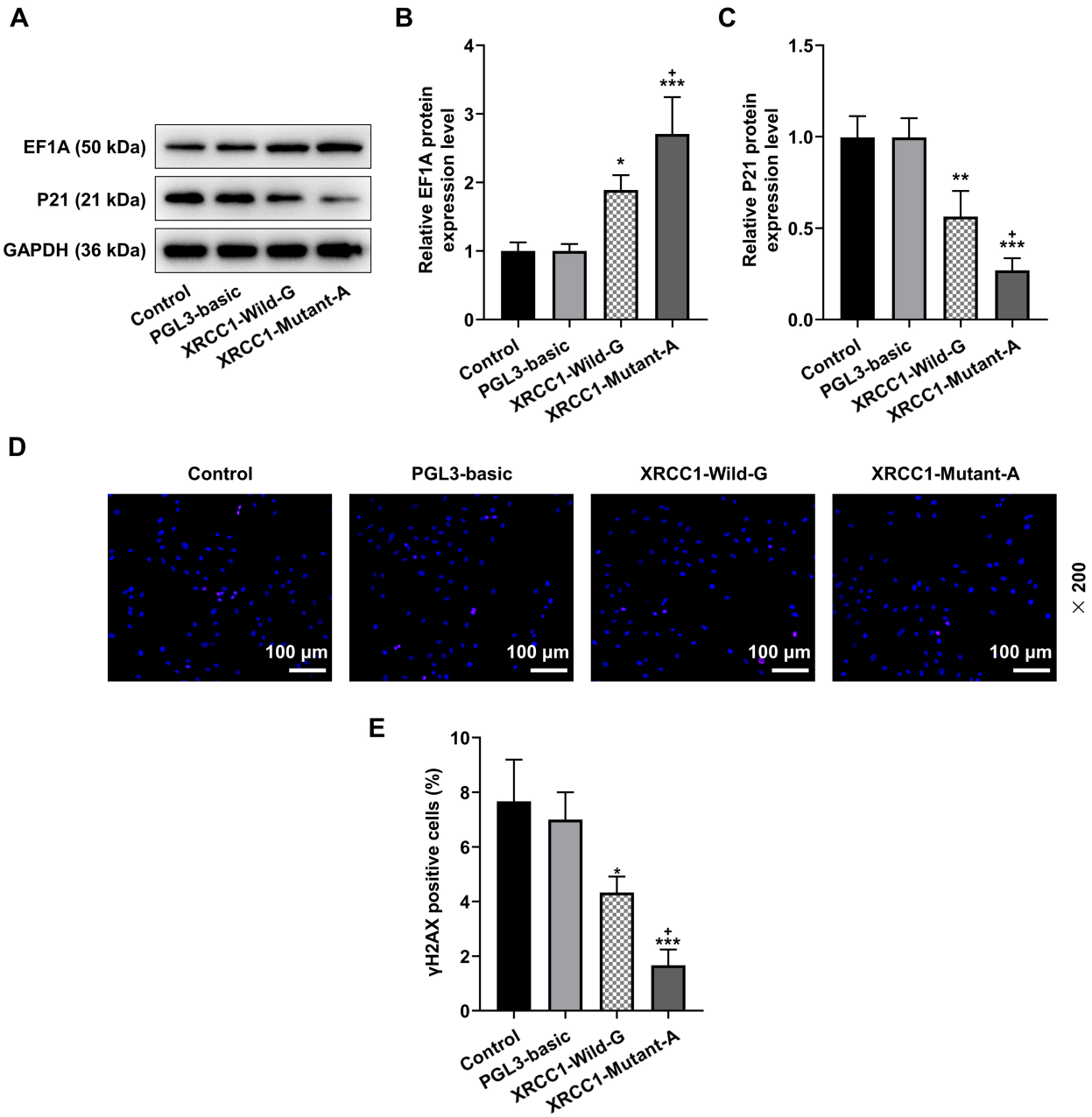

Fig. 2. rs1799782 mutation of *XRCC1* regulated the expressions of senescence-related proteins and *γH2AX* focus formation. (A–C) Expression levels of senescence-related proteins P21 and EF1A (Western blot). GAPDH was employed as the internal control. (D,E) Representative immunofluorescent images of *γH2AX* foci in A549 cells (200×). Scale bar = 100 μm. *γH2AX* was positive for secondary antibody (red), and the cell nuclei was positive for DAPI (blue). $^{*}p < 0.05$, $^{**}p < 0.01$, $^{***}p < 0.001$ vs. PGL3-basic. $^{+}p < 0.05$ vs. XRCC1-Wild-G. Quantified values from at least three independent repeated experiments (n = 3) were exhibited as mean ± standard deviation. GAPDH, glyceraldehyde-3-phosphate dehydrogenase; *γH2AX, phosphorylated H2A.X variant histone*; DAPI, 4,6-diamidino-2-phenylindole.

Wild-G group (Fig. 1E,F, $p < 0.01$). Among senescence-related proteins, we observed that EF1A protein expression was elevated, yet P21 expression was lessened in the XRCC1-Mutant-A and XRCC1-Wild-G groups, with more pronounced increase and decrease in the XRCC1-Mutant-A group (Fig. 2A–C, $p < 0.05$). Next, we detected the expression of *γH2AX* by immunofluorescence to assess the DNA damage of cells. Our data demonstrated that XRCC1-Mutant-A led to a significant decrease in the formation of *γH2AX* foci in LC cells (Fig. 2D,E, $p < 0.05$).

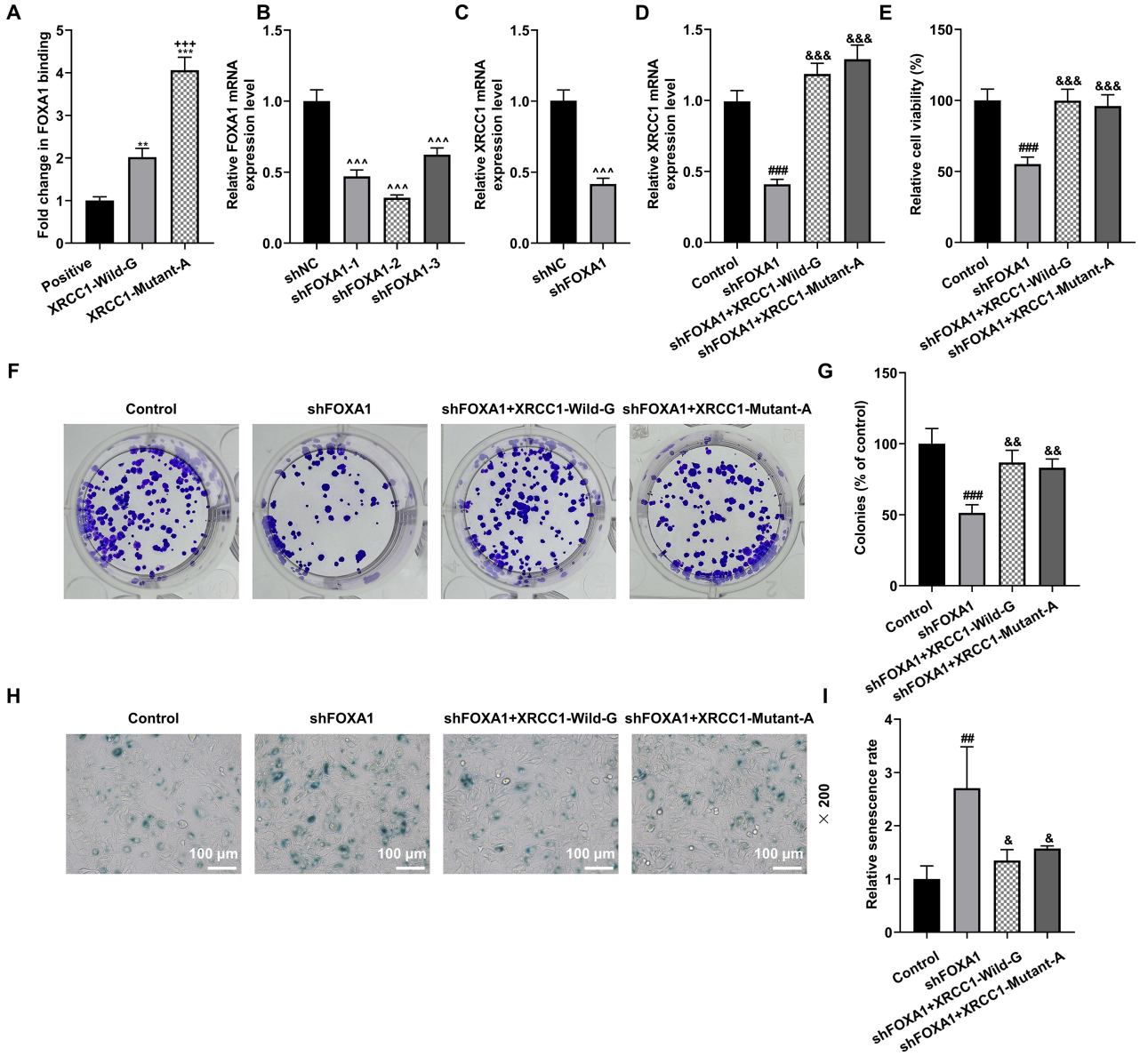

Fig. 3. Impacts of *XRCC1* mutation and sh*FOXA1* upon the viability, colony formation and senescence of LC cells. (A) ChIP assay was performed on the chromatin obtained from cells transfected with XRCC1-Wild-G or XRCC1-Mutant-A, using qRT-PCR, with GAPDH as the internal control. (B) The transfection efficiency of sh*FOXA1*-1, sh*FOXA1*-2 and sh*FOXA1*-3 in LC cells (qRT-PCR). (C) The expression of *XRCC1* in LC cells transfected with sh*FOXA1*-1 (qRT-PCR). (D–I) LC cells were transfected with sh*FOXA1*-1 and XRCC1-Wild-G/XRCC1-Mutant-A. (D) The expression of *XRCC1* in LC cells (qRT-PCR). (E) The viability of LC cells (CCK-8 assay). (F,G) The colony formation ability of LC cells (colony formation assay). (H,I) Cellular senescence (SA-β-gal staining assay; magnification: $\times$200, and scale bar = 100 μm). $^{**}p < 0.01$, $^{***}p < 0.001$ vs. Positive. $^{+++}p < 0.001$ vs. XRCC1-Wild-G. $^{\wedge\wedge\wedge}p < 0.001$ vs. shNC. $^{\#\#}p < 0.01$, $^{\#\#\#}p < 0.001$ vs. Control. $^{\&}p < 0.05$, $^{\&\&}p < 0.01$, $^{\&\&\&}p < 0.001$ vs. sh*FOXA1*. Quantified values from at least three independent repeated experiments (n = 3) were presented as mean $\pm$ standard deviation. ChIP, Chromatin Immunoprecipitation; qRT-PCR, quantitative reverse transcription polymerase chain reaction; sh*FOXA1*, *FOXA1*-specific short hairpin RNA.

shFOXA1 Reversed the Effects of XRCC1-Mutant-A or XRCC1-Wild-G on Viability, Colony Formation and Senescence of LC Cells

ChIP assay was performed to validate whether *XRCC1* mutation could affect the binding affinity of *FOXA1* and *XRCC1*, the result which indicated that XRCC1-Mutant-A showed a stronger binding affinity to *FOXA1* than XRCC1-Wild-G (Fig. 3A, $p < 0.001$). We then designed three kinds of sh*FOXA1*, and verified their inhibition efficiency on *FOXA1* by quantitative reverse transcription polymerase chain reaction (qRT-PCR) (Fig. 3B, $p < 0.001$). Based on the results, sh*FOXA1*-2 was retained for subsequent experi-

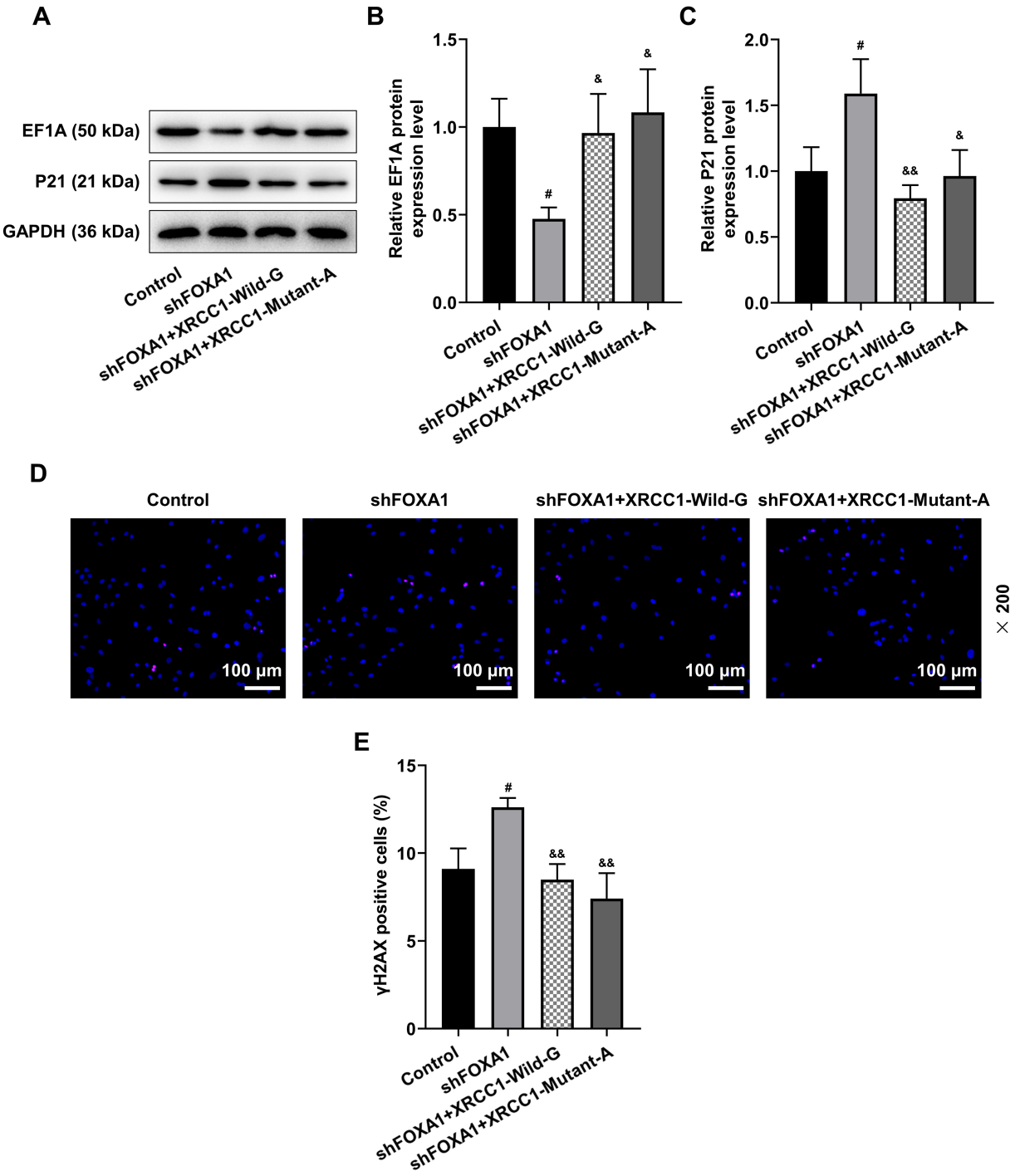

Fig. 4. Effects of *XRCC1* mutation and sh*FOXA1* on expressions of senescence-related proteins and *γH2AX* focus formation. LC cells were transfected with sh*FOXA1*-1 and XRCC1-Wild-G/XRCC1-Mutant-A. (A–C) Expression levels of senescence-related proteins P21 and EF1A (Western blot). GAPDH was employed as the internal control. (D,E) Representative immunofluorescent images of *γH2AX* foci in A549 cells (200×). Scale bar = 100 μm. *γH2AX* was positive for secondary antibody (red), and the cell nuclei was positive for DAPI (blue). $^{\#}p < 0.05$ vs. Control. $^{\&}p < 0.05$, $^{\&\&}p < 0.01$ vs. sh*FOXA1*. Quantified values from at least three independent repeated experiments (n = 3) were denoted as mean ± standard deviation.

ments. sh*FOXA1* decreased *XRCC1* expression (Fig. 3C,D, $p < 0.001$), cell viability and colony number (Fig. 3E–G, $p < 0.001$), and promoted senescence of LC cells (Fig. 3H,I, $p < 0.01$). However, XRCC1-Mutant-A or XRCC1-Wild-G reversed the effects of sh*FOXA1* on *XRCC1* expression, viability, colony formation and senescence of LC cells (Fig. 3D–I, $p < 0.05$).

shFOXA1 Offset the Effects of XRCC1-Mutant-A or XRCC1-Wild-G on Expressions of Senescence-Related Proteins and γH2AX Focus Formation in LC Cells

sh*FOXA1* resulted in the downregulation of EF1A protein and the upregulation of P21 protein (Fig. 4A–C, $p < 0.05$). Furthermore, the promoted *γH2AX* focus formation was also observed in the shFOXA1 group (Fig. 4D,E). However, the impacts of sh*FOXA1* upon senescence-related proteins and *γH2AX* focus formation were offset by XRCC1-Mutant-A or XRCC1-Wild-G (Fig. 4A–E, $p < 0.05$).

Discussion

In recent years, *XRCC1* gene polymorphisms, including rs1799782, rs25489 and rs25487, have been successively found to be associated with increased risk of LC [16,17]. However, few studies have focused on the molecular mechanism by which the *XRCC1* gene polymorphism promotes LC development. Here, we demonstrated that the enhanced binding of rs1799782 and *FOXA1* can upregulate *XRCC1* transcription and thus elevate the risk of LC.

The protein encoded by *XRCC1* acts as a scaffold for other proteins in the DNA repair complex, so as to make a critical impact on DNA damage [18]. DNA damage brought on by endogenous/exogenous substances can hinder cancer cell proliferation, and therefore, cancer cells can use *XRCC1* to recover proliferation ability [19]. Zhangyong Yin *et al.* [20] pointed out that *XRCC1*-mediated DNA repair ability can protect LC cells from cisplatin-mediated damage, while inhibiting *XRCC1* expression can make LC cells sensitive to cisplatin. As the study by Neelum Aziz Yousafzai *et al.* [21] revealed, with the elevation of *XRCC1* expression, that the expression of *γH2AX* (a DNA damage marker) in LC cells is decreased; similar results were also obtained in this study, except that we found that the XRCC1-Mutant-A possesses much stronger repair ability than XRCC1-Wild-G.

In addition, we also studied the effect of *XRCC1* on the senescence of LC cells. Continued DNA damage will affect cell senescence and increase the risk of cancer [22]. The senescence of cancer cells is a favorable barrier to prevent tumor occurrence [23]. P21, as a biomarker of cell senescence, can induce reactive oxygen species production to further trigger cell senescence [24]. Moreover, the tumor protein p53 (P53)-P21 pathway is one of the main pathways that can induce cancer cell senescence [25]. The research of Hongmei Luo *et al.* [26] emphasized that *EF1A* expression is downregulated in aging LC cells treated with resveratrol. Consistent with previous studies, our results revealed that XRCC1-Mutant-A and XRCC1-Wild-G inhibit the expression of SA-β-gal and P21, but promote the expression of EF1A, indicating that XRCC1-Mutant-A and XRCC1-Wild-G both can suppress cell senescence. However, XRCC1-Mutant-A has a stronger inhibitory effect on cell senescence than XRCC1-Wild-G. To the best of our knowledge, this is the first research revealing the effects of rs1799782 on LC cell senescence.

Next, we focused on the relationship between *FOXA1* and *XRCC1*. ChIP assay results demonstrated that XRCC1-Mutant-A has a stronger binding affinity with *FOXA1* compared to XRCC1-Wild-G, thus enhancing the transcription of *XRCC1* with the help of *FOXA1*. A similar mechanism has been previously reported in cervical cancer [8]. Several studies have proved that *FOXA1* is a vital transcription factor in the occurrence and development of LC, and its overexpression can enhance cell metastasis and proliferation [27,28]. However, the effect of *FOXA1* on LC cell aging has not been reported, but previous study showed that the expression of *FOXA1* was negatively correlated with the aging marker IL-6 level [29]. Further, Yusuke Imamura *et al.* [30] reported that the depletion of *FOXA1* can increase P21 expression in prostate cancer cells. In this study, we verified through rescue experiments that sh*FOXA1* can reverse the effects of XRCC1-Mutant-A on the viability, colony formation and senescence of LC cells. This demonstrated that XRCC1-Mutant-A enhances expression of *XRCC1* by binding to *FOXA1*, and then plays a role in DNA repair of LC cells, ultimately leading to LC development.

Conclusions

This study revealed that the mechanism by which rs1799782 increases LC risk is related to *FOXA1*-mediated enhancement of *XRCC1* transcription. In the future, therefore, LC patients with *XRCC1* rs1799782 polymorphism might be treated by *FOXA1* inhibitors or drugs that block the binding of rs1799782 with *FOXA1*. However, more *in vivo* experiments are needed to confirm the results.

Availability of Data and Materials

The analyzed data sets generated during the study are available from the corresponding author upon reasonable request.

Author Contributions

CLX and YLL designed the research study; JWP, SHW, ZTY and XPC performed the research; HZ, ZYY and ZC collected and analyzed the data. All authors have been involved in drafting the manuscript and all authors have been involved in revising it critically for important intellectual content. All authors give final approval of the version to be published. All authors have participated sufficiently in the work to take public responsibility for appropriate portions of the content and agreed to be accountable for all aspects of the work in ensuring that questions related to its accuracy or integrity.

Ethics Approval and Consent to Participate

Not applicable.

Acknowledgment

Not applicable.

Funding

This work was supported by Zhejiang Medical and Health Research Project [2023RC314] and [2024KY576], [2023KY1376] and [2021KY1235]; and Longquan Science and Technology Bureau Project [2021KJ-004] and Lishui Science and Technology Bureau Project [2020077571].

Conflict of Interest

The authors declare no conflict of interest.

References

[1] Bade BC, Dela Cruz CS. Lung Cancer 2020: Epidemiology, Etiology, and Prevention. Clinics in Chest Medicine. 2020; 41: 1–24.

[2] Benusiglio PR, Fallet V, Sanchis-Borja M, Coulet F, Cadranel J. Lung cancer is also a hereditary disease. European Respiratory Review. 2021; 30: 210045.

[3] Shen H, Zhu M, Wang C. Precision oncology of lung cancer: genetic and genomic differences in Chinese population. NPJ Precision Oncology. 2019; 3: 14.

[4] Liu S, Xiao Y, Hu C, Li M. Associations between polymorphisms in genes of base excision repair pathway and lung cancer risk. Translational Cancer Research. 2020; 9: 2780–2800.

[5] London RE. XRCC1 - Strategies for coordinating and assembling a versatile DNA damage response. DNA Repair. 2020; 93: 102917.

[6] Nissar B, Kadla SA, Khan NS, Shah IA, Majid M, Afshan FU, *et al*. DNA Repair Gene XRCC1 and XPD Polymorphisms and Gastric Cancer Risk: A Case-Control Study Outcome from Kashmir, India. Analytical Cellular Pathology. 2018; 2018: 3806514.

[7] Degtyareva AO, Antontseva EV, Merkulova TI. Regulatory SNPs: Altered Transcription Factor Binding Sites Implicated in Complex Traits and Diseases. International Journal of Molecular Sciences. 2021; 22: 6454.

[8] Meng Q, Wang S, Tang W, Wu S, Gao N, Zhang C, *et al*. XRCC1 mediated the development of cervival cancer through a novel Sp1/Krox-20 swich. Oncotarget. 2017; 8: 86217–86226.

[9] He Y, Wang L, Wei T, Xiao YT, Sheng H, Su H, *et al*. FOXA1 overexpression suppresses interferon signaling and immune response in cancer. The Journal of Clinical Investigation. 2021; 131: e147025.

[10] Wang X, Yin Y, Du R. SOX9 dependent FOXA1 expression promotes tumorigenesis in lung carcinoma. Biochemical and Biophysical Research Communications. 2019; 516: 236–244.

[11] Rahmanian N, Shokrzadeh M, Eskandani M. Recent advances in γH2AX biomarker-based genotoxicity assays: A marker of DNA damage and repair. DNA Repair. 2021; 108: 103243.

[12] Chen SL, Lu SX, Liu LL, Wang CH, Yang X, Zhang ZY, *et al*. eEF1A1 Overexpression Enhances Tumor Progression and Indicates Poor Prognosis in Hepatocellular Carcinoma. Translational Oncology. 2018; 11: 125–131.

[13] Takasugi M, Yoshida Y, Hara E, Ohtani N. The role of cellular senescence and SASP in tumour microenvironment. The FEBS Journal. 2023; 290: 1348–1361.

[14] McQuin C, Goodman A, Chernyshev V, Kamentsky L, Cimini BA, Karhohs KW, *et al*. CellProfiler 3.0: Next-generation image processing for biology. PLoS Biology. 2018; 16: e2005970.

[15] Livak KJ, Schmittgen TD. Analysis of relative gene expression data using real-time quantitative PCR and the 2(-Delta Delta C(T)) Method. Methods. 2001; 25: 402–408.

[16] Wang X, Ma KW, Zhao YG, Wang GJ, Li W. XRCC1 rs25487 polymorphism is associated with lung cancer risk in epidemiologically susceptible Chinese people. Genetics and Molecular Research. 2015; 14: 15530–15538.

[17] Choudhary A, Anand A, Singh A, Roy P, Singh N, Kumar V, *et al*. Machine learning-based ensemble approach in prediction of lung cancer predisposition using XRCC1 gene polymorphism. Journal of Biomolecular Structure & Dynamics. 2023. (online ahead of print)

[18] Caldecott KW. XRCC1 protein; Form and function. DNA Repair. 2019; 81: 102664.

[19] Iyama T, Wilson DM, 3rd. DNA repair mechanisms in dividing and non-dividing cells. DNA Repair. 2013; 12: 620–636.

[20] Yin Z, Chen E, Cai X, Gong E, Li Y, Xu C, *et al*. Baicalin attenuates XRCC1-mediated DNA repair to enhance the sensitivity of lung cancer cells to cisplatin. Journal of Receptor and Signal Transduction Research. 2022; 42: 215–224.

[21] Yousafzai NA, Zhou Q, Xu W, Shi Q, Xu J, Feng L, *et al*. SIRT1 deacetylated and stabilized XRCC1 to promote chemoresistance in lung cancer. Cell Death & Disease. 2019; 10: 363.

[22] Stead ER, Bjedov I. Balancing DNA repair to prevent ageing and cancer. Experimental Cell Research. 2021; 405: 112679.

[23] Calcinotto A, Kohli J, Zagato E, Pellegrini L, Demaria M, Alimonti A. Cellular Senescence: Aging, Cancer, and Injury. Physiological Reviews. 2019; 99: 1047–1078.

[24] Huang W, Hickson LJ, Eirin A, Kirkland JL, Lerman LO. Cellular senescence: the good, the bad and the unknown. Nature Reviews. Nephrology. 2022; 18: 611–627.

[25] Kumari R, Jat P. Mechanisms of Cellular Senescence: Cell Cycle Arrest and Senescence Associated Secretory Phenotype. Frontiers in Cell and Developmental Biology. 2021; 9: 645593.

[26] Luo H, Yang A, Schulte BA, Wargovich MJ, Wang GY. Resveratrol induces premature senescence in lung cancer cells via ROS-mediated DNA damage. PLoS ONE. 2013; 8: e60065.

[27] Li J, Zhang S, Zhu L, Ma S. Role of transcription factor FOXA1 in non small cell lung cancer. Molecular Medicine Reports. 2018; 17: 509–521.

[28] Li J, Zhang Y, Wang L, Li M, Yang J, Chen P, *et al*. FOXA1 prevents nutrients deprivation induced autophagic cell death through inducing loss of imprinting of IGF2 in lung adenocarcinoma. Cell Death & Disease. 2022; 13: 711.

[29] Hu W, Li M, Wang Y, Zhong C, Si X, Shi X, *et al*. Comprehensive bioinformatics analysis reveals the significance of forkhead box family members in pancreatic adenocarcinoma. Aging. 2023; 15: 92–107.

[30] Imamura Y, Sakamoto S, Endo T, Utsumi T, Fuse M, Suyama T, *et al*. FOXA1 promotes tumor progression in prostate cancer via the insulin-like growth factor binding protein 3 pathway. PLoS ONE. 2012; 7: e42456.